Journal of Mining and Earth Sciences

Website: http://jmes.humg.edu.vn

Application of Remote Sensing Imagery and Algorithms in Google Earth Engine platform for Drought Assessment

Hoa Thanh Thi Pham *, Ha Thanh Tran

Hanoi University of Mining and Geology, Hanoi, Vietnam

ARTICLE INFO

Article history:
Received 26th Dec. 2020
Revised 14th Apr. 2021
Accepted 22nd May 2021

Keywords:
Drought,
Google Earth Engine,
Remote sensing,
Tay Hoa,
VHI.

ABSTRACT

In Vietnam, drought is one of the natural disasters caused by high temperatures and lack of precipitation, especially with El Nino and the global warming phenomenon. It affects directly environmental, economical, social issues, and the lives of humans. Many methods have been used to assess drought, in which remote sensing indices are considered the most commonly used tool today. They are used to analyze spatio-temporal distribution of drought conditions and identify drought severity. Especially with the launch of Google Earth Engine (GEE) - a cloud-based platform for geospatial analysis, it is easy to access high-performance computing resources for processing multi-temporal satellite data online. With the GEE platform, we focus on writing and running scripts with the indicators suitable for evaluating drought phenomenon, instead of calculating on software and downloading remote sensing imagery with large size. In this study, we collected 26 Landsat 8 images in the dry season in 2019 (from April to July) in Tay Hoa district, Phu Yen – a region in the South Central Coast of Vietnam where agricultural drought occurs frequently. We assessed the distribution of drought conditions by using a drought index (VHI index – Vegetation Health Index) produced from Landsat satellite data in the GEE platform. The study results indicated that the drought (from mild to severe) concentrated in the North of the region, corresponding to high surface temperature and NDVI low or NDVI moderate values. VHI maps were visually compared with the drought map of the South Central Coast and the Central Highlands. In general, the results also reflect the the method's reliability and can be used to support the managers to plan policies, making long-term plans to cope with climate change in the future at Tay Hoa in particular and other regions in general.

*Corresponding author
E-mail: phamthithanhhoa@humg.edu.vn
DOI: 10.46326/JMES.2021.62(3).07

1. Introduction

In recent times, climate change are the main reasons which caused global warming, the lack of rainfall, making the drought more serious. This phenomenon greatly impacts agriculture such as reducing crop productivity, reducing cultivated areas and crop yields, mainly food crops. Therefore, identifying of drought extent is considered an important program to assess the drought occurrence and its severity to agriculture development in Vietnam.

Although drought types occur at different timescales as usual, it is detected in the dry season with precipitation shortages, high temperatures (Wilhite, 2000). Besides, it often happens in large areas. Therefore, many scientists worldwide have recognized the potential of using indices observed from remote sensing data to monitor drought effectively. The main reason was given as remote sensing technology provides a synoptic view of the Earth's surface. The advantage of technology is that image data is delivered continuously over time and whole the globe, so the details of the results are shown legibly with different regions, more efficient than the measurement with the monitoring point. The use of remote sensing data to establish drought maps will provide an overview of the space of drought areas for the regions where there are no or few meteorological stations and there is a variety of free satellite imagery suitable for evaluating drought conditions, such as MODIS and LANDSAT.

Among drought indices derived from remote sensing data, the Normalized Difference Vegetation Index (NDVI) combined with Land Surface Temperature (LST) provides a strong correlation. It gives valuable information to identify agricultural drought (Sruthi et al., 2015). Based on NDVI and LST relationship, many drought indices were introduced, such as Temperature – Vegetation Dryness Index (TVDI), Vegetation Health Index (VHI), Water Supplying Vegetation Index (WSVI), and tested successfully in many countries (Alshaikh, 2015; Schirmbeck et al., 2017; Sholihah et al., 2016). VHI demonstrated a greater capability and better suitability in monitoring drought (Bento et al., 2018). It combines two indices: Vegetation Condition Index (VCI) and Temperature Condition Index (TCI). VCI is used to measure changes in NDVI and TCI determined the difference of LST over time. Globally, many studies were conducted for the assessment of drought intensity by application this index with Landsat imagery (Masitoh et al., 2019; Sreekesh et al., 2019). In Vietnam, this index was applied in the research of (Nguyen Viet Lanh et al., 2018; Tran et al., 2017). Thus, it can be seen that the availability of remote sensing data with wide space coverage has enabled scientists to study drought phenomenon around the globe.

Especially, thanks to the launch of Google Earth Engine (GEE) - a cloud-based platform for geospatial analysis, it is easy to access high-performance computing resources for processing multi-temporal satellite data online (Gorelick et al., 2017). Since its appearance in 2010, GEE abilities have been utilized for many applications (Mutanga et al., 2019), including vegetation mapping and monitoring, land cover/ land cover change mapping (Midekisa et al., 2017; Sidhu et al., 2018), flood mapping (DeVries et al., 2020; Sunar et al., 2019). Besides, GEE with a large amount of freely available satellite imagery and direct image processing has been considered a potential application in drought studies (Aksoy et al., 2019; Khan et al., 2019; Sazib et al., 2018). Space and temporal analysis have been flexibly done on this platform. The availability of global soil moisture data of the GEE data catalog and web-based tools were used in the study (Sazib et al., 2018) to enable users to assess the impact of drought quickly and easily. Meanwhile, Aksoy et al., (2019) analyzed the temporal distribution of drought conditions in Turkey within 20 years using different drought indices, such as Vegetation Health Index (VHI), Normalized Multiband Drought Index (NMDI), and Normalized Difference Drought Index (NDDI). These indices are produced from MODIS satellite data in the GEE platform. Similar to (Aksoy et al., 2019), algorithms on GEE were chosen to calculate indices: Vegetation Condition Index (VCI), Precipitation Condition Index (PCI), Soil Moisture Condition Index (SMCI), and Temperature Condition Index (TCI) (Khan et al., 2019). These results showed that MODIS - derived indices provide helpful spatial information for assessing drought conditions from the regional level to the country level. Significantly, they demonstrated that the tools on GEE allow easy analysis and visualization. These tools help explore spatial and temporal variations in information and drought conditions for any location in the world with processing or managing data to a minimum, instead of working with image processing software on laptop or computer which are often time-consuming and labor-intensive.

In Vietnam, the research of GEE is still relatively new. The applications have focused on forest land monitoring (Nguyen Trong Nhan et al., 2018; Nhut et al., 2018), river bank changes (Long et al., 2019), and flood monitoring (Tuan et al., 2018). However, few studies evaluate drought using medium resolution imagery such as Landsat in GEE in Vietnam. Therefore, in this study, satellite-based drought indices of NDVI, LST, VCI, TCI, VHI are calculated in the GEE using algorithms and Landsat 8 in the local level to assess drought conditions in the dry season in 2019. The results of the research may provide the initial information about drought hazards for authorities and regional planners.

2. Materials

2.1. Study Area

The study area is Tay Hoa – a rural district of Phu Yen Province in the South Central Coastal region of Vietnam (Figure 1).

There are main types of terrain, including mountains and plain. The hilly regions are in the South, stretching from the West to the East, accounting for over 50% of the natural area. The West area is a red basalt land with an average elevation of 30÷40 m, suitable for developing short and long-term industrial crops. The plain is located to the North and the East, in which the East area is alluvial land, a large rice-growing plain of Phu Yen Province.

Like some other localities in the region, Tay Hoa has a tropical monsoon climate, hot and humid, and is influenced by ocean climate. There are two distinct seasons: the rainy season from September to December and the dry season from

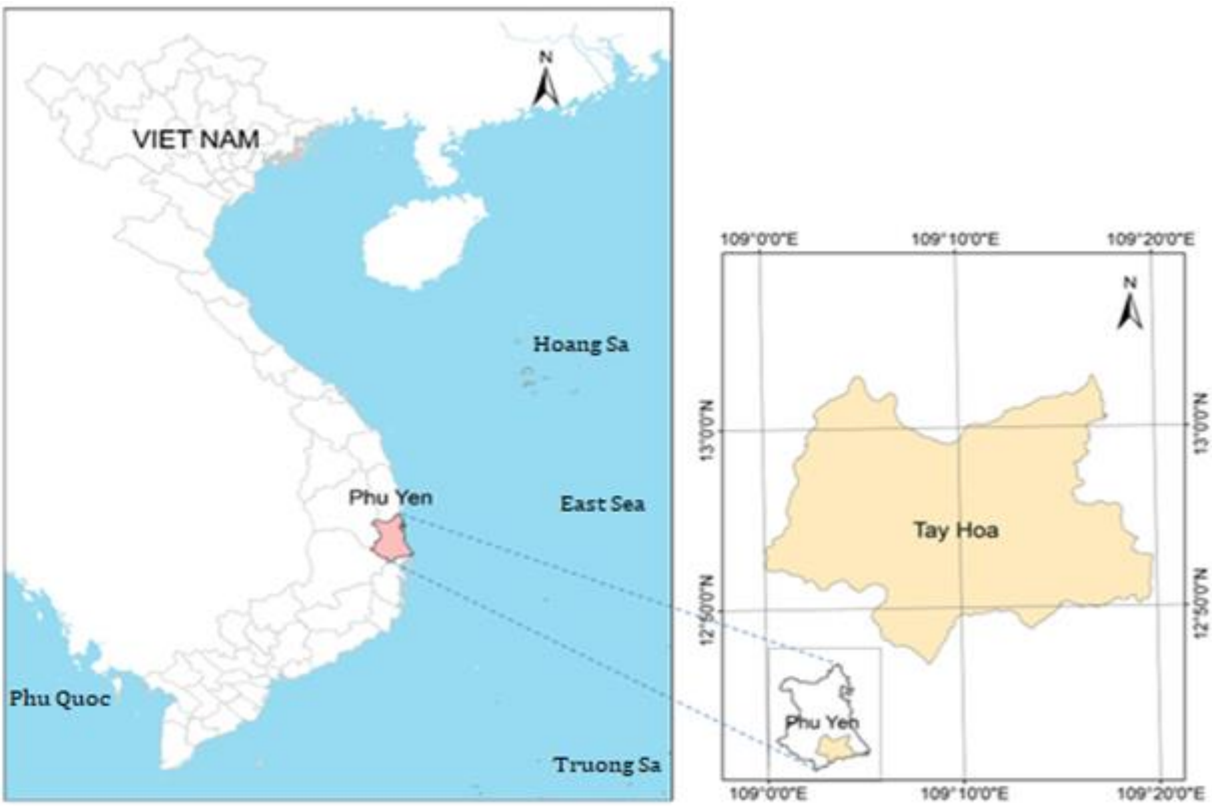

Figure 1. Location of the study area.

January to August (Department of Natural Resources and Environment of Phu Yen Province, 2019).

For the past few years, the drought situation in Tay Hoa has been complicated. Significantly, the dry season in 2019 had the most severe recorded drought. The prolonged severe drought and sweltering weather have dried up hundreds of hectares of crops and forests. Because of the hot weather and strong southwest wind, hundreds of hectares of eucalyptus forest were destroyed. Many communes could not practice agriculture due to water scarcity, and many households lack water. (Online Vietnam Agriculture Newspaper, 2019)

2.2. Data resources

Earth Engine provides an enormous amount of data from satellites hosted by Google. Each data source available on GEE has Image Collection and ID (The data in GEE can be looked up at GEE catalog via website https://earthengine.google.com/datasets/). In which, Landsat 8 imagery was added recently when its satellite was launched in 2013, with a 16-day repeat cycle and resolution of imagery from 15 meters (Panchromatic) to 100 meters (Thermal Infrared), the average one is 30 meter with multispectral data. All Landsat 8 data are directly available to GEE, including Tier 1, Tier 2, raw scenes, top-of-atmosphere (TOA), and surface reflectance (SR) data. All thermal bands have been resampled to 30 m spatial resolution.

Table 1 describes the Landsat data in this study. All Landsat 8 images which were covered entirely the district, were retrieved from the 2019. Tier 1 data (T1) have the highest radiometric and positional quality and are recommended for all time-series analysis (by USGS). TOA data were converted from raw digital numbers values using the calibration coefficients from the image metadata (Chander et al., 2009). The SR data were generated using the Land Surface Reflectance Code (LaSRC) algorithm (Vermote et al., 2016). The TIR band from the TOA data, the Red and Near-infrared (NIR) bands from the SR data were chosen for spatial processing analysis to compute LST and NDVI. The Landsat 8 image series was shown in section 4.

2.3. Google Earth Engine

Google Earth Engine is available via a web-based JavaScript Application Program Interface (API) called the Code Editor.

The center panel provides a JavaScript code editor. The map in the bottom panel contains the layers added by the script. The left panel contains code examples, your saved scripts in Scripts tab. The Docs tab of the Code Editor lists the methods of each API class. The Asset Manager is in the Assets tab in the left panel, is used to upload and manage your image assets in Earth Engine. Code Editor scripts can be shared via an encoded URL. (https://developers.google.com/earth-engine)

There are several ways to run operations in the API: Calling methods attached to objects, Calling algorithms, Calling Code Editor specific functions, and Defining new roles. The Google Earth Engine API provides a library of functions that may be applied to data for display and analysis.

Table 1. List of products in the GEE catalog used in the study.

ID	Description	Used Bands	Spatial Resolution	Date range
LANDSAT/LC08/C01/T1_TOA	Landsat 8, Collection 1, Tier1, TOA (top-of-atmosphere reflectance)	TIR	100m, resampled to 30 m.	From April to July 2019
LANDSAT/LC08/C01/T1_SR	Landsat 8, Collection 1, Tier1, SR (surface reflectance)	NIR, Red	30 m	

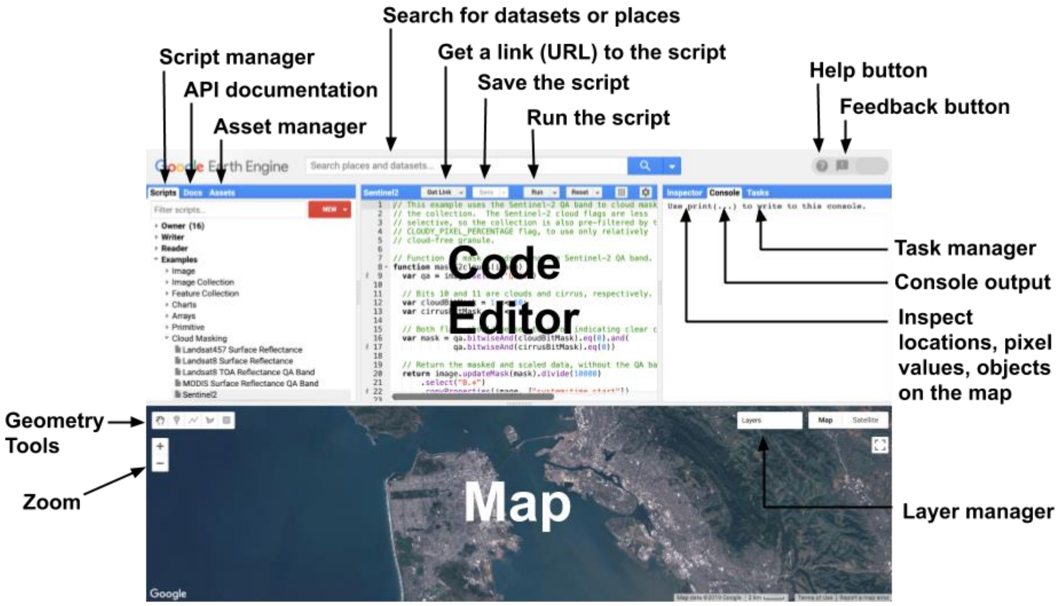

Figure 2. Diagram of components of the Earth Engine Code Editor at code.earthengine.google.com. (Source: https://developers.google.com/earth-engine).

3. Methodology

With the GEE platform, we used the algorithms/ functions to write and execute scripts for indices as mention before in section 1: Normalized Difference Vegetation Index (NDVI), Land Surface Temperature (LST), Vegetation Condition Index (VCI), Temperature Condition Index (TCI), and Vegetation Health Index (VHI). The red and the near-infrared bands (respectively, bands 4 and 5) of Landsat 8 are used to construct NDVI while the thermal band calculates LST. From these indices, three other indices as VCI, TCI, and VHI, were derived. All math formulas were presented in sections 3.2 and 3.3.

3.1. The image processing and analysis in GEE for drought assessment

Figure 3 illustrates the processing chain for generating the VHI index for drought assessment. Our processing workflow consists of some steps using coding by the JavaScript (JS) API:

1. Loading input data

- Load the collections of Landsat 8 TOA and SR: using function ***ee.Image()***;

- Load the study area with shapefile format: using **Table Upload** in the **Assets tab**.

2. Filter images by date range and the region of interest: using ***filterDate()*** and ***filterBounds()***.

3. Remove the cloud from the TOA and SR images using a module cloud mask with QA band.

4. Clip images according to the boundary of the study area: using the ***clip(geometry)***.

5. NDVI was calculated with the existing image processing function in GEE: ***normalizedDifference(bandNames)***.

6. LST, VCI, TCI, and VHI were computed by creating ***expression()*** with operators as ***Add, Subtract, Multiply, Divide***.

3.2. Formulas for calculating NDVI and LST indices

- NDVI quantifies vegetation by measuring the difference between near-infrared (which vegetation strongly reflects) and red light (which vegetation absorbs). The range of NDVI is −1 to +1. The higher value of NDVI refers to healthy and dense vegetation. Lower NDVI values show sparse vegetation. The NDVI is calculated as follows (Tucker, 1979):

$$NDVI = \frac{NIR - RED}{NIR + RED} \qquad (1)$$

Where:

RED and NIR stand for the spectral reflectance measurements acquired in the red (visible) and near-infrared regions, respectively.

- LST (Land Surface Temperature) estimation using the following equation (Weng et al., 2004):

$$LST = \frac{T_B}{1 + \left(\frac{\lambda . T_B}{\rho}\right) * \ln LSE} \quad (2)$$

Land Surface Temperature (LST) was derived from the Top of Atmosphere Brightness Temperature (T_B) for the Landsat's thermal infrared (TIR) channels which are provided by the United States Geological Survey (USGS) and are fully available and ready to use in GEE for Landsat 8, collection 1.

Besides, The LST retrieval algorithm used here requires prescribed values of Land Surface Emissivity (LSE). Values of LSE were calculated based on the proportion of vegetation Pv. The following formula is used:

$$LSE = 0.004P_V + 0.986 \quad (3)$$

Whereas, Pv combined with NDVI are often used as parameters to assess the emissivity while lacking actual ground emissivity data. Pv is calculated according to (Sobrino et al., 2004):

$$P_V = \left(\frac{NDVI - NDVI_{min}}{NDVI_{max} - NDVI_{min}}\right)^2 \quad (4)$$

In equation (2), ρ = 14380, ρ = h*c/s with h is Plank's constant ($6{,}626*10^{-34}$ Js), s is Boltzmann's constant ($1{,}38*10^{-23}$ J/K); c is velocity of light ($3*10^{8}$ m/s).

3.3. VCI, TCI and VHI calculation

Vegetation Condition Index (VCI) is a derived index from NDVI values. The VCI is expressed in % from 0 to 100, with low values representing stressed vegetation conditions, middle values representing fair conditions, and high values representing optimal or above-normal conditions (Kogan, 1995). Meanwhile, Temperature Condition Index (TCI) was created because surface temperature is higher in dry years and derived from the change of surface temperature in a specific time series. TCI determines the stress on vegetation caused by temperatures and shows different vegetation responses.

The Vegetation Health Index (VHI) was estimated using VCI and TCI for all observed times (Kogan, 1995).

$$VCI = 100 \times \frac{NDVI - NDVI_{min}}{NDVI_{max} - NDVI_{min}} \quad (5)$$

$$TCI = 100 \times \frac{LST_{max} - LST}{LST_{max} - LST_{min}} \quad (6)$$

$$VHI = a \times VCI + (1 - a) \times TCI \quad (7)$$

Where:

NDVI and LST - NDVI and LST values of each month in the dry season in 2019;

NDVI max and NDVI min - the maximum and minimum value of NDVI;

LST max and LST min - the maximum and minimum value of LST.

A and (1-a) are coefficients showing the difference in weighting between VCI and TCI in total vegetation health. The value of "a" depends on different conditions of environment and climate. In unknown environmental conditions, "a" is selected as 0.5 correspondings to the average condition, assuming an equal contribution of both variables to the combined index (Kogan, 2000). VHI values were divided into 5 classes as, Table 2 (Kogan, 1995).

4. Results and discussion

Using GEE, we were able to produce data quickly. From April to July 2019, 13 Landsat 8

Table 2. Drought level distribution following (Kogan, 1995).

No	VHI value	Drought level
1	<10	Extreme drought
2	10÷20	Severe drought
3	20÷30	Moderate drought
4	30÷40	Mild drought

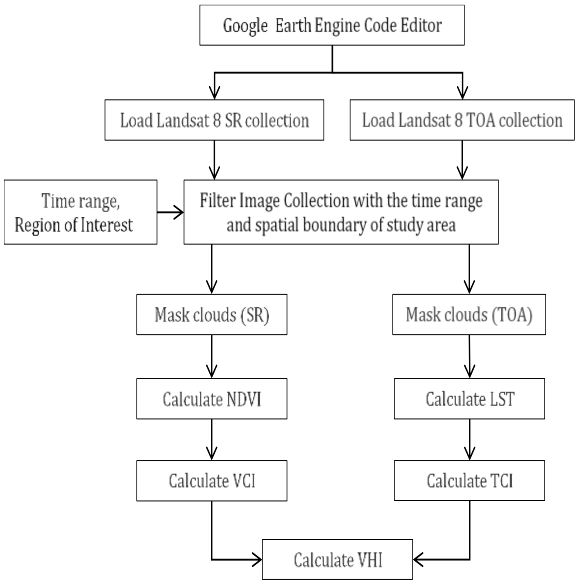

Figure 3. The flowchart of image processing and analyzing in the GEE platform for retrieving Vegetation Health Index VHI.

TOA images and 13 Landsat 8 SR images were collected by coding. Figure 4 shows the Code Editor scripts to extract drought indices from satellite images. On the other hand, the VHI image was also displayed directly in the Code Editor interface (in the Layer section), the values (NDVI min and max, LST min and max), chart of LST-NDVI correlation presented in the Console section. Final output tiff files (NDVI, LST, VCI, TCI, VHI images) were in Tasks section and exported to google drive.

4.1. NDVI, LST and LST-NDVI correlation

Using the LST–NDVI scatterplot in GEE, a linear regression model was constructed to determine the relationship between LST and NDVI in the dry season. Correlation analysis has been done to determine the relationship between LST and NDVI, shown in Figure 5: the relationship changed from month to month, a strong negative correlation in April 2019 with the coefficient of determination R2 (The total variance) 0.812.

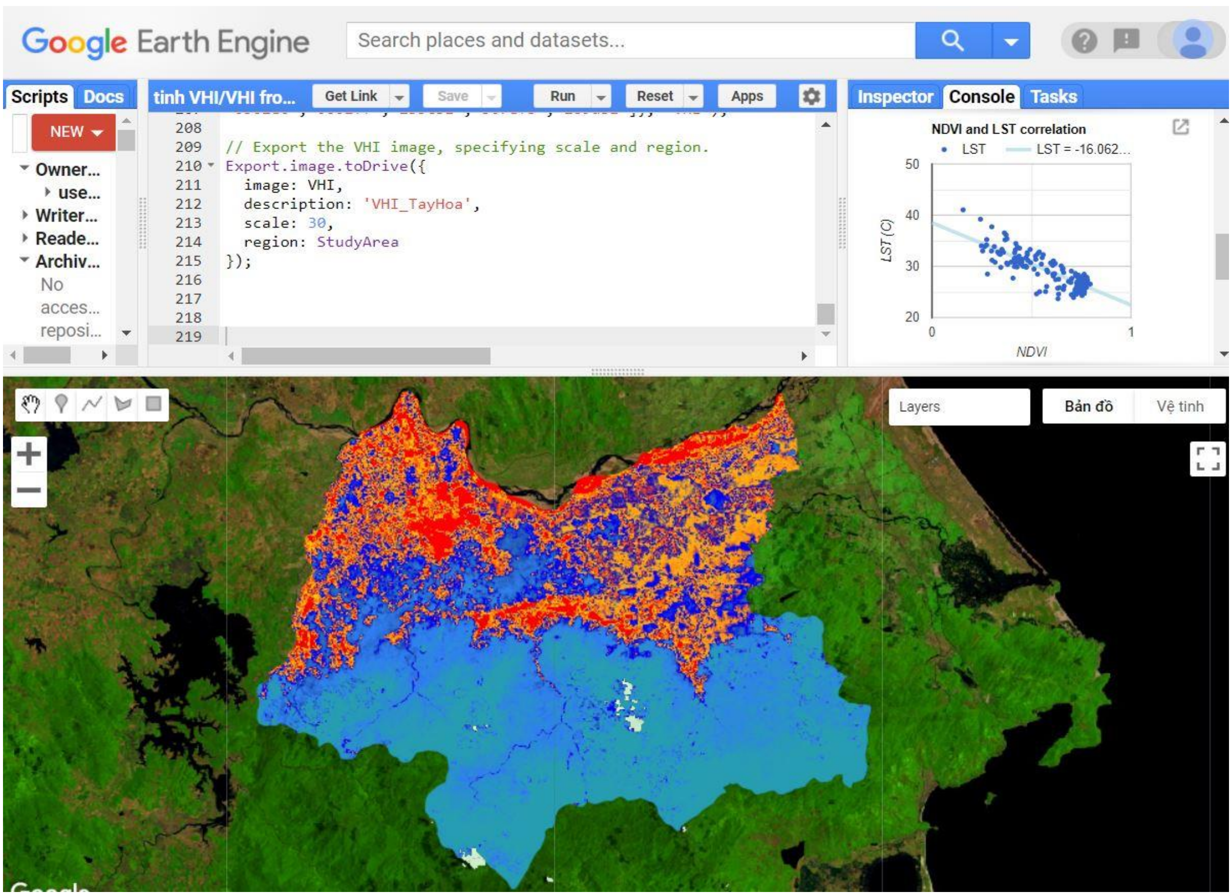

Figure 4. Results in GEE.

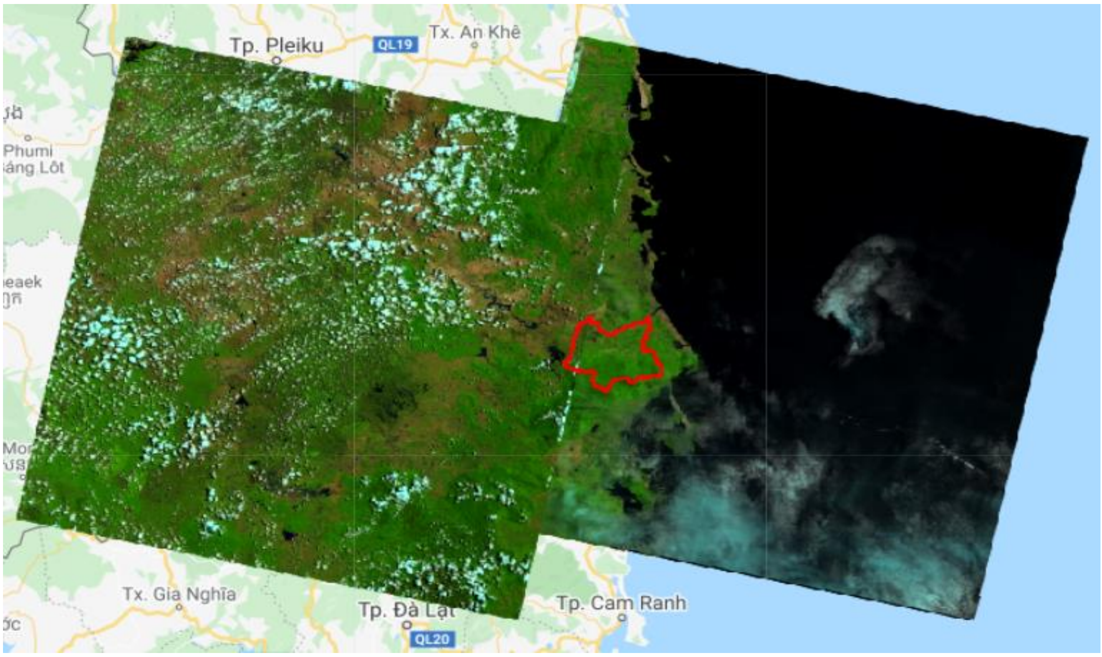

Figure 5. Landsat 8 images of the study area from April to July 2019 in GEE (The false color composite uses a band combination of SWIR-1 (B6), near-infrared (B5), blue (B4). The study area is outlined in red.

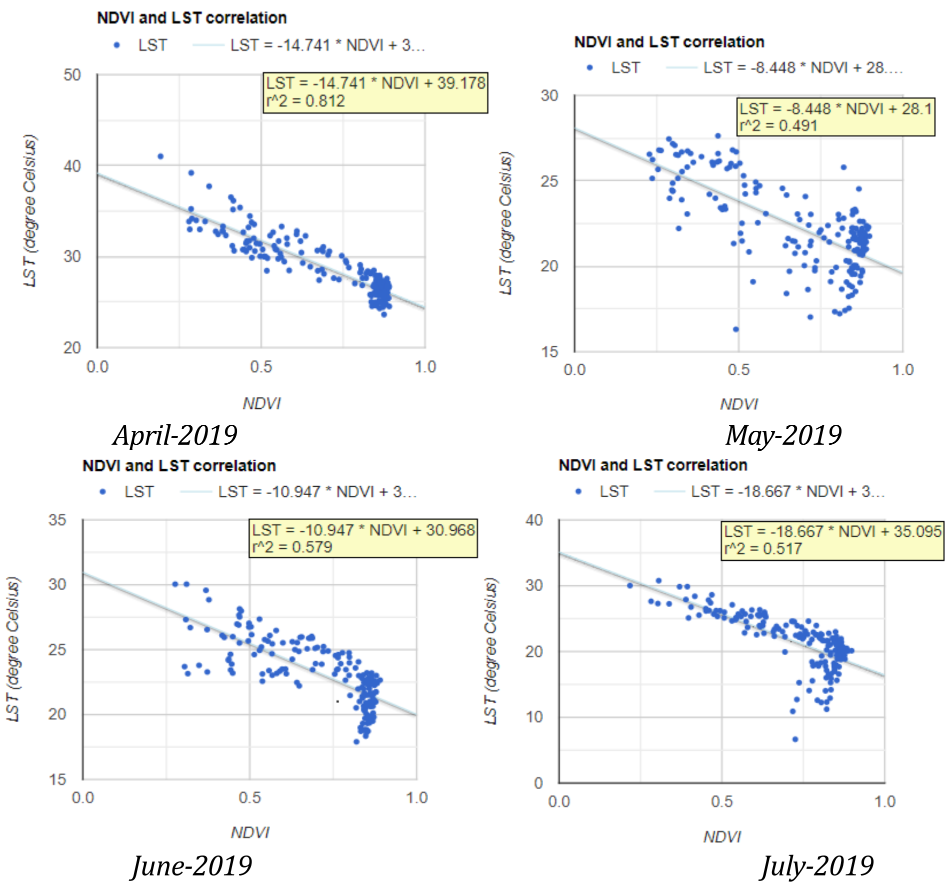

Figure 6. LST-NDVI correlation.

Generally, the NDVI-LST regression showed a moderate fit (>0.5), exception of May 2019 (R2 was 0.491). However, the linear equation in May 2019 still presents the inverse relation between LST and NDVI. The previous studies have also found similar results (Ferrelli et al., 2018; Gorgani et al., 2013). From these studies, it is evaluated that the land surface temperature is high where the vegetation cover is found low. Thus, this study also confirms that the land surface temperatures are higher and increase more markedly in areas of sparse vegetation cover. Conversely, dense vegetation cover absorbs the land surface temperature.

The spatial distributions of LST and NDVI are illustrated in Figure 7. High values of NDVI indicate the information of health, dense vegetation, and lower values represented stressed vegetation. Negative values correspond to areas with water surfaces. Overall, in Tay Hoa, the distribution of high NDVI values was in the South (the green area), corresponds to the forest, the density of vegetation declined in the North (yellow and red area). During the dry season, nearly the entire studied area had surface temperatures higher than 20°C. Especially in April 2019, the surface temperature is mainly greater than 25^0C (orange and red color), in which the highest temperature is above 42^0C. Comparison between NDVI and LST images from April to July 2019, in areas where high LST values were observed, the NDVI diminished due to the variation in vegetation state. Overall, they are also considered tools for monitoring drought periods. NDVI at a given pixel will typically be relatively low, whereas LST is expected to be relatively high because of vegetation deterioration.

4.2. Spatial drought

Figure 8 represents the spatial distribution of VCI, TCI, and VHI. TCI and VCI were created based on the condition that the higher the temperature, the worse the conditions for vegetation. High values of VCI signify good vegetation; on the contrary, its values decrease to 0 show extremely unfavorable vegetation conditions. Low TCI values indicate harsh weather conditions (due to high temperatures), and high values (close to 100) reflect mostly favorable conditions.

Generally, the results show TCI, VCI, and VHI had a similar pattern from April to July in 2019, with values close to 0 in the North and values increase to 100 in the South of the studied area. Moreover, the distribution of drought phenomenon over the dry season period in 2019 is shown in Figure 9 with four levels: from no drought to severe (white to red, respectively). The forests are distributed in the South of Tay Hoa district and were not affected by drought (VHI values >40). From April to July 2019, the vulnerable to drought areas tended to increase, mainly in Son Thanh Dong, Son Thanh Tay, Hoa My Dong, Hoa Binh 1, Hoa Binh 2, and Hoa Phong, where land is used for agriculture (by overlaying VHI map with land use map of Tay Hoa). Besides, the total drought area is recorded for 17÷20% of the entire district, corresponding to the site with high surface temperature from $25 \div 30^0$C and NDVI low or NDVI moderate values (Figure 7). Overall, the VHI index is chosen to assess the drought of vegetation caused by temperature. Therefore, it is appropriate to indicate the extent of agricultural drought.

To assess the accuracy of the results of agricultural drought using the VHI index by coding in the GEE platform, we made the following comparisons:

1. Due to the limitation of observational data in the study area, we compared LST images in the study with LST from MOD11A1 V6 data which were provided directly on GEE (see https://developers.google.com/earth-engine/datasets/catalog/MODIS_006_MOD11A1?hl=en). The comparison results between retrieved LST from Landsat 8 and Modis LST revealed a good correlation (values R2 > 0.67). Although the comparison is not entirely valid because the resolution of the MOD11A1 V6 product is low, it shows that free Landsat 8 imagery sources helpd calculate LST approprivately in small areas.

2. Comparing drought conditions between VHI index map of Tay Hoa district with the Palmer map (PDSI - Palmer Drought Severity Index) of the South Central Coast and the Central Highlands. This map was published in 2016 and was a result of the project of Vietnam Academy for Water

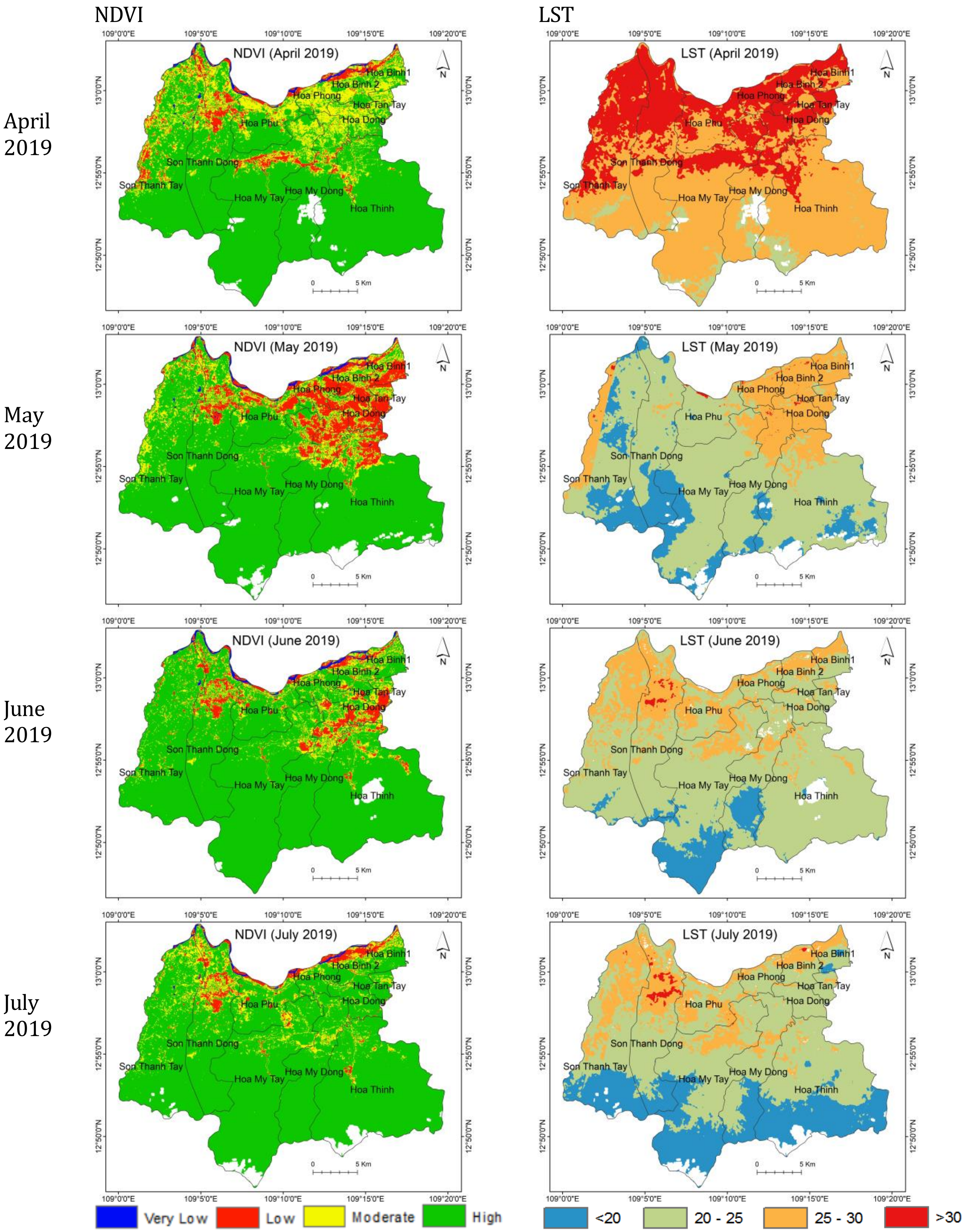

Figure 7. Spatial variation of NDVI and LST in April – July 2019.

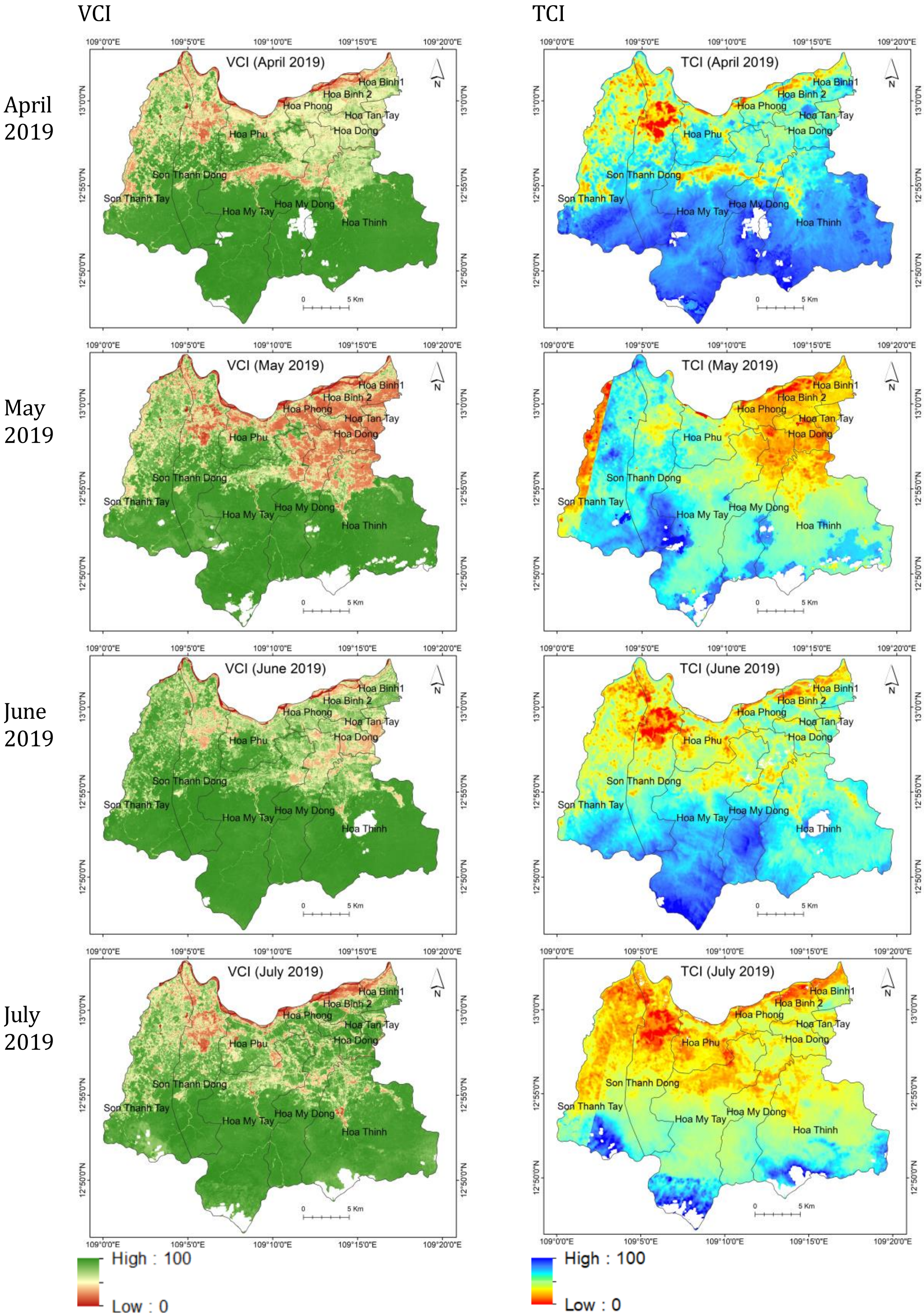

Figure 8. VCI and TCI in Tay Hoa district in dry season 2019.

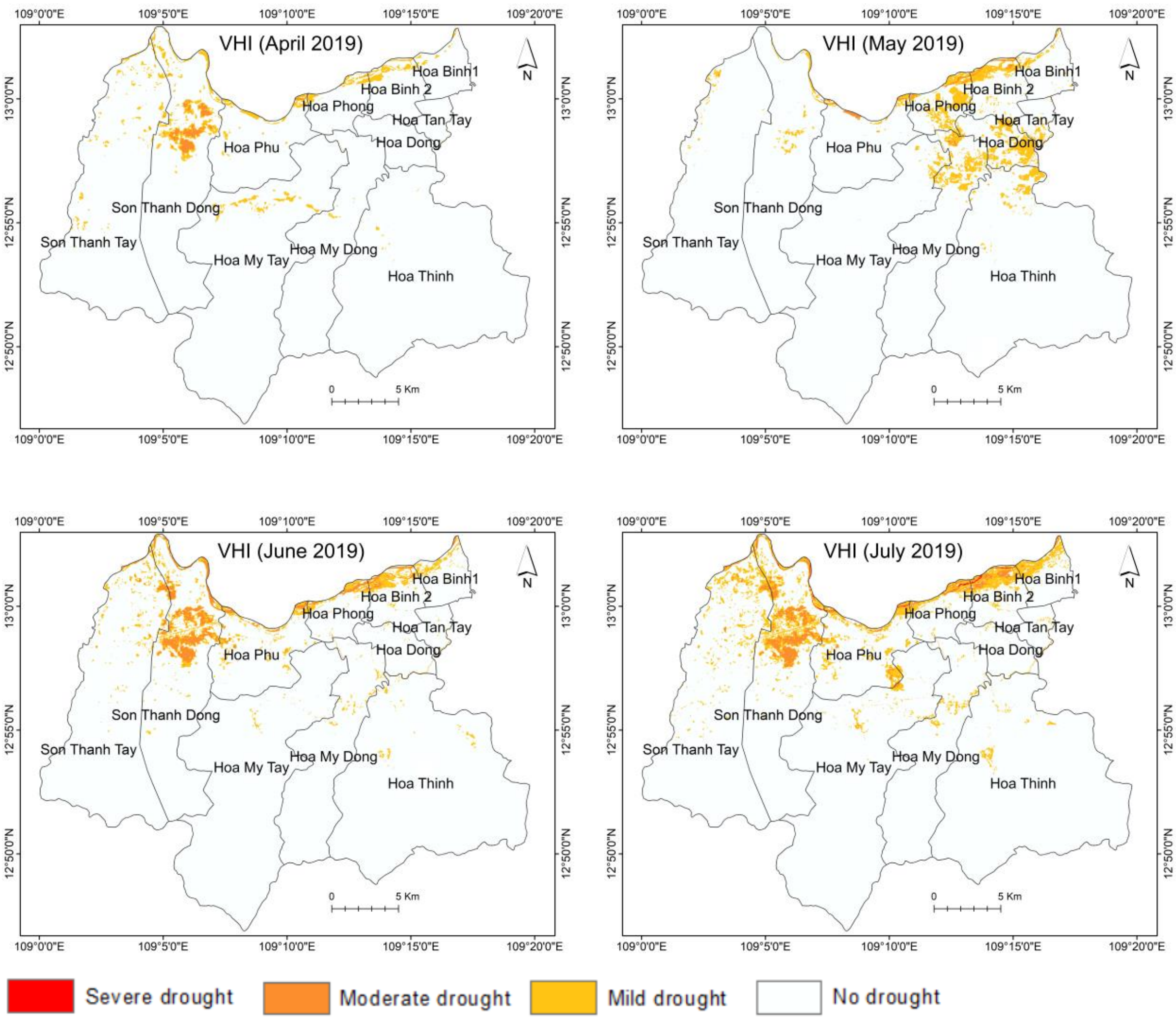

Figure 9. Spatial distribution of drought with VHI index.

Resource. While VHI uses LST and NDVI extracted from remote sensing for monitoring agricultural drought, PDSI uses readily available temperature and precipitation data series (Alley, 1984; Palmer, 1965). The drought in 2016 occurred in most provinces of the south - central coast and the central highlands in general and Tay Hoa district in particular, while the drought results in 2019 in the study mainly occurred in the northern regions of Tay Hoa. Although there are no similarities in space, time and index, the comparison is also found that drought area in 2019, also existed in 2016. Besides, we overlayed the VHI map with the land use map of Tay Hoa. Therefore, the results of the areas identified as drought are consistent with the reality of crop regions. Overall, the results also reflect the method's reliability, especially in the absence of meteorological information in the area.

5. Conclusion

This study assessed drought conditions in a relatively small rural area in the south - central coastal of Vietnam during the dry season. The method relies on Google Earth Engine and algorithms/scripts to analyze and calculate the Vegetation Health Index (VHI) - drought index. Our results confirm that from April to July 2019, the preliminary information about the spatial distribution of mild, moderate, and severe drought in the Tay Hoa district was provided quickly. Futhermore, it shows the potential of using GEE to monitor drought. The GEE data catalog includes all the Landsat imagery and replaces all the heavy computational processes with advanced cloud computing technologies, the results obtained for a short time. The Google Earth

Engine methodology that we developed in this research will contribute to assessing and monitoring drought for Tay Hoa district.

However, this method also has the disadvantages: it depends on selecting of suitable Landsat 8 images for the study area. Images with a large cloud cover will not be selected because the information about drought at this time will be lost. Therefore, to solve this combining different types of satellite imagery in GEE (Landsat, Sentinel, Modis) and adding the parameters to indicate drought conditions, such as water capacity and rainfall.

Acknowledgment

The authors would like to thank the Hanoi University of Mining and Geology for funding this research in Project No T20-10.

Author contributions

Pham Thi Thanh Hoa: Conceived the idea, performed the analytic calculations, wrote the manuscript. Tran Thanh Ha: analyzed the data and formulas, commented and edited this manuscript.

References

Aksoy, S., Gorucu, O.,Sertel, E. (2019). Drought Monitoring using MODIS derived indices and Google Earth Engine Platform. *Paper presented at the 2019 8th International Conference on Agro-Geoinformatics (Agro-Geoinformatics)*. 1-6. doi: 10.1109/Agro-Geoinformatics.2019.8820209.

Alley, W. (1984). The Palmer Drought Severity Index: Limitations and Assumptions. *Journal of Climate and Applied Meteorology, 23*, 1100-1109. doi: 10.1175/1520-0450(1984)023<1100:TPDSIL>2.0.CO;2.

Alshaikh, A. Y. (2015). Space applications for drought assessment in Wadi-Dama (West Tabouk), KSA. *The Egyptian Journal of Remote Sensing and Space Science, 18*(1, Supplement 1), S43-S53. doi: https://doi.org/10.1016/j.ejrs.2015.07.001.

Bento, V., Gouveia, C., Dacamara, C.,Trigo, I. (2018). A climatological assessment of drought impact on vegetation health index. *Agricultural and Forest Meteorology, 259*, 286-295. doi: 10.1016/j.agrformet.2018.05.014.

Chander, G., Markham, B. L.,Helder, D. L. (2009). Summary of current radiometric calibration coefficients for Landsat MSS, TM, ETM+, and EO-1 ALI sensors. *Remote Sensing of Environment, 113*(5), 893-903. doi: https://doi.org/10.1016/j.rse.2009.01.007.

Department of Natural Resources and Environment of Phu Yen Province, (2019). *Climate assessment reports of Phu Yen province* (in Vietnamese).

DeVries, B., Huang, C., Armston, J., Huang, W., Jones, J.,Lang, M. (2020). Rapid and robust monitoring of flood events using Sentinel-1 and Landsat data on the Google Earth Engine. *Remote Sensing of Environment, 240*. doi: 10.1016/j.rse.2020.111664.

Ferrelli, F., Huamantinco Cisneros, M., Delgado, A.,Piccolo, M., (2018). Spatial and temporal analysis of the LST-NDVI relationship for the study of land cover changes and their contribution to urban planning in Monte Hermoso, Argentina. *Documents d'Anàlisi Geogràfica, 64*, 25. doi: 10.5565/rev/dag.355.

Gorelick, N., Hancher, M., Dixon, M., Ilyushchenko, S., Thau, D.,Moore, R. (2017). Google Earth Engine: Planetary-scale geospatial analysis for everyone. *Remote Sensing of Environment, 202*, 18-27. doi: https://doi.org/10.1016/j.rse.2017.06.031.

Gorgani, S., Panahi, M.,Rezaie, F. (2013). The Relationship between NDVI and LST in the urban area of Mashhad, Iran. *Paper presented at the International Conference on Civil Engineering Architecture & Urban Sustainable Development. At Tabriz , Iran*.

Khan, R., Gilani, H., Iqbal, N.,Shahid, I. (2019). Satellite-based (2000–2015) drought hazard assessment with indices, mapping, and monitoring of Potohar plateau, Punjab, Pakistan. *Environmental Earth Sciences, 79*(1), 23. doi: 10.1007/s12665-019-8751-9.

Kogan, F. N. (1995). Application of vegetation index and brightness temperature for drought detection. *Advances in Space Research, 15*(11), 91-100. doi: https://doi.org/10.1016/0273-1177(95)00079-T.

Kogan, F. N. (2000). Satellite-Observed Sensitivity of World Land Ecosystems to El Niño/La Niña. *Remote Sensing of Environment, 74*, 445-462. doi: 10.1016/S0034-4257(00)00137-1.

Long, V. H., Giang, N. V., Hoanh, T. P.,Hoa, P. V., (2019). Applying Google Earth Engine in river bank erosion monitoring – a case study in lower Mekong river (in Vietnamese). *Journal of science- Ho Chi Minh city University of Education*.

Masitoh, F., & Rusydi, A. N. (2019). Vegetation Health Index (VHI) analysis during drought season in Brantas Watershed. *IOP Conference Series: Earth and Environmental Science, 389*, 012033. doi: 10.1088/1755-1315/389/1/012033.

Midekisa, A., Holl, F., Savory, D. J., Andrade-Pacheco, R., Gething, P. W., Bennett, A.,Sturrock, H. J. W. (2017). Mapping land cover change over continental Africa using Landsat and Google Earth Engine cloud computing. *PLOS ONE, 12*(9), e0184926. doi: 10.1371/journal.pone.0184926.

Mutanga, O.,Kumar, L. (2019). Google Earth Engine Applications. *Remote Sensing, 11*, 591. doi: 10.3390/rs11050591.

Nguyen Trong Nhan, Cuong, V. X. (2018). Google Earth Engine was applied to forest land monitoring in Lam Dong province from 2010 - 2016 (in Vietnamese). *The fourth Scientific Conference - SEMREGG 2018*, 258-265.

Nguyen Viet Lanh, Dung, N. V., Duong, T. H., Tam, T. T. (2018). Using satellite precipitation data to assess meteorological drought based on SPI index for Thanh Hoa province. *Vietnam Journal of Hydro - Meteorology, 696*, 1-9.

Nhut, H. S., Hoa, P. V., Binh, N. A., An, N. N., Phuong, T. A.,Thao, G. T. P. (2018). Using Google Earth Engine for assessing mangrove forest change in Ngoc Hien district, Ca Mau province in the period 2000-2015 (in Vietnamese). *Journal of science- Ho Chi Minh city University of Education, 15*(11b), 101-107.

Online Vietnam Agriculture Newspaper. (2019). https://nongnghiep.vn/phu-yen-han-han-khoc-liet-mot-xa-thieu-nuoc-nghiem-trong-d247764.html.

Palmer, W. C. (1965). *Meteorological Drought.* Research Paper No. 45, US Weather Bureau, Washington, DC.

Sazib, N., Mladenova, I.,Bolten, J. (2018). Leveraging the Google Earth Engine for Drought Assessment Using Global Soil Moisture Data. *Remote Sensing, 10*, 1265. doi: 10.3390/rs10081265.

Schirmbeck, L. W., Fontana, D. C., Schirmbeck, J., Mengue, V. P. (2017). Understanding TVDI as an index that expresses soil moisture. *Journal of Hyperspectral Remote Sensing, 7*, 82-90.

Sholihah, R., Trisasongko, B., Shiddiq, D., Iman, L. O., Kusdaryanto, S., Manijo,Panuju, D. (2016). Identification of Agricultural Drought Extent Based on Vegetation Health Indices of Landsat Data: Case of Subang and Karawang, Indonesia. *Procedia Environmental Sciences, 33*, 14-20. doi: 10.1016/j.proenv.2016.03.051

Sidhu, N., Pebesma, E.,Câmara, G. (2018). Using Google Earth Engine to detect land cover change: Singapore as a use case. *European Journal of Remote Sensing, 51*, 486-500. doi: 10.1080/22797254.2018.1451782

Sobrino, J. A., Jiménez-Muñoz, J. C.,Paolini, L. (2004). Land surface temperature retrieval from LANDSAT TM 5. *Remote Sensing of Environment, 90*(4), 434-440. doi: https://doi.org/10.1016/j.rse.2004.02.003.

Sreekesh, S., Kaur, N.,Sreerama Naik, S. R. (2019). Agricultural drought and soil moisture analysis using satellite image based indices. *Int. Arch. Photogramm. Remote Sens. Spatial Inf. Sci., XLII-3/W6*, 507-514. doi: 10.5194/isprs-archives-XLII-3-W6-507-2019.

Sruthi, S.,Aslam, M. A. M. (2015). Agricultural Drought Analysis Using the NDVI and Land Surface Temperature Data; a Case Study of Raichur District. *Aquatic Procedia, 4*, 1258-1264. doi: https://doi.org/10.1016/j.aqpro.2015.02.164

Sunar, F., Yağmur, N.,Dervisoglu, A. (2019). Flood Analysis with Remote Sensing Data - a Case Study: Maritsa River, Edirne. *ISPRS - International Archives of the Photogrammetry, Remote Sensing and Spatial Information Sciences, XLII-3/W8*, 497-502. doi: 10.5194/isprs-archives-XLII-3-W8-497-2019.

Tran, H. T., Campbell, J. B., Tran, T. D.,Tran, H. T. (2017). Monitoring drought vulnerability using multispectral indices observed from sequential remote sensing (Case Study: Tuy Phong, Binh Thuan, Vietnam). *GIScience & Remote Sensing, 54*(2), 167-184. doi: 10.1080/15481603.2017.1287838.

Tuan, V. Q., Khai, D. H., Nhan, H. T. K., Hoa, N. T. (2018). Development of flood monitoring algorithms in the Mekong Delta based on Google Earth Engine platform (in Vietnamese). *Can Tho University Journal of Science, 54*(9A), 29-36.

Tucker, C. J. (1979). Red and photographic infrared linear combinations for monitoring vegetation. *Remote Sensing of Environment, 8*(2), 127-150. doi: https://doi.org/10.1016/0034-4257(79)90013-0.

Vermote, E., Justice, C., Claverie, M., Franch, B. (2016). Preliminary analysis of the performance of the Landsat 8/OLI land surface reflectance product. *Remote Sensing of Environment, Volume 185*(2), 46-56. doi: 10.1016/j.rse.2016.04.008.

Weng, Q., Lu, D.,Schubring, J. (2004). Estimation of land surface temperature–vegetation abundance relationship for urban heat island studies. *Remote Sensing of Environment, 89*(4), 467-483. doi: https://doi.org/10.1016/j.rse.2003.11.005.

Wilhite, D. (2000). Drought as a Natural Hazard: Concepts and Definitions. *Drought, a Global Assessment, 1*.